

An expectation-based space-time scan statistic for ZIP-distributed data

Benjamin Allévius¹ and Michael Höhle¹

¹Department of Mathematics, Stockholm University, Sweden

Chapter Abstract

An expectation-based scan statistic is proposed for the prospective monitoring of spatio-temporal count data with an excess of zeros. The method, which is based on an outbreak model for the zero-inflated Poisson distribution, is shown to be superior to traditional scan statistics based on the Poisson distribution in the presence of structural zeros. The spatial accuracy and detection timeliness of the proposed scan statistic is investigated by means of simulation, and an application on weekly cases of Campylobacteriosis in Germany illustrates how the scan statistic could be used to detect emerging disease outbreaks. An implementation of the method is provided in the open source R package `scanstatistics` available on CRAN.

Keywords: EM algorithm, disease surveillance, scan statistic, spatio-temporal, zero-inflated Poisson.

1 Introduction

The resurgence of infectious diseases such as Ebola and Zika in recent years has put the efforts of public health agencies in the spotlight. These agencies often monitor several hundred different pathogens as they are reported by local clinics and hospitals across a country. The movement of both people and foodstuff within and between countries enables diseases to spread quickly and can cause outbreaks that affect many locations simultaneously. By the joint surveillance of data from multiple geographical areas, be they different countries or smaller regions within a single country, conducted with regular frequency (e.g. weekly), public health agencies hope to detect such outbreaks and identify the affected areas in a timely manner (Salmon et al., 2016a; Cakici et al., 2010). One group of methods utilized for this purpose are *scan statistics*. The aim of this paper is to introduce a novel scan statistic for space-time data, prove its effectiveness relative to alternatives, and provide a reference to an implementation of the proposed method.

Scan statistics are used to detect clusters in spatial and spatio-temporal datasets, and have been applied in fields as diverse as astronomy (Moni Bidin et al., 2009), ecology (Tuia et al., 2008), and criminology (Minamisava et al., 2009). The primary use of scan statistics continues to be in public health surveillance, however, and this is the area of application we will focus on to demonstrate the method proposed in this paper. Scan statistics detect clusters by first *scanning* over regions of interest, calculating *statistics* for all potential clusters. The scan statistic is then obtained as the maximum of these statistics, and the corresponding *most likely cluster* (MLC) thus identified. To determine whether such a cluster was detected as a result of an emerging outbreak or because of chance occurrence, formal hypothesis testing can be conducted. Typically, P -values or rejection regions are obtained through the use of Monte Carlo methods.

A common assumption for many scan statistics, such as those proposed by Kulldorff (1997), Gangnon and Clayton (2001), Tango and Takahashi (2005), and Li et al. (2011), is that the observed number of events in a given area and time period follows a Poisson distribution. This distribution is a natural first choice for rare event data or for count data with a large or unclear upper bound. However, scan statistics that rely on the Poisson assumption have been criticized on two points in particular: their inability to capture overdispersion in the data (Tango et al., 2011; de Lima et al., 2015) and their inability to handle zero-inflated counts (Cançado et al., 2014; de Lima et al., 2015). Additionally, a debate has recently flared up around the use of traditional scan statistics, such as those implemented in the software SATSCANTM (Kulldorff, 2016), and the hypothesis testing procedures used

when carrying out prospective analyzes (Correa et al., 2015a; Kulldorff and Kleinman, 2015; Correa et al., 2015b). Essentially, the issue discussed is if and how both past and future analyzes should be accounted for when deciding which significance level to use for the analysis at hand. In the latest contribution to the debate, Tango (2016) argues that Correa et al. (2015a) are right but on the wrong grounds. Reiterating the point made in Tango et al. (2011), he asserts that prospective analyzes should not be conducted using conditional expected counts, i.e. conditional on the total number of observed cases. Rather, all baseline parameters should be estimated independently of the current study period, on past data that is believed to be free from disease outbreaks and other anomalies. In the nomenclature of Neill (2006), Tango (2016) argues that prospective analysis should be conducted with *expectation-based* scan statistics, not *population-based* scan statistics.

Motivated by the need for expectation-based scan statistics and the inability of many current scan statistics to handle excess zeros, we take inspiration from the work of Cañado et al. (2014) and propose an expectation-based prospective scan statistic for spatio-temporal counts governed by a zero-inflated Poisson (ZIP) distribution. The proposed scan statistic along with several others are made available in the open-source R package `scanstatistics`, which can be seen as a complement to the SATSCANTM (Kulldorff, 2016) software and its R interface `rsatscan` (Kleinman, 2015), as well as to more general disease surveillance packages such as `surveillance` (Salmon et al., 2016b).

The structure of this paper is as follows: In Section 2, the theoretical basis and assumptions of an outbreak model based on the ZIP distribution is described, and algorithms for parameter estimation and calculation of the proposed scan statistic are given. Section 3 then describes a simulation study conducted to test the performance of the method relative to another scan statistic. This is followed by an application on *Campylobacter* data in Section 4. Finally, conclusions and major takeaways are given in Section 5.

2 Methods

Counts of zero are not rare in applications, and can come about in several ways. In disease surveillance, for example, zero cases may be reported for a given area and time period because none of the ill individuals decided to visit the doctor, and this chance circumstances is in some sense responsible for these cases remaining undetected. We refer to such zero counts as *sampling zeros*. Quite a different reason to see a count of zero is that no disease was present, and assuming no false positives, consequently no cases were

recorded. This latter type of observation, which cannot be anything but zero, will be referred to as a *structural zero*. A more deceptive variant of a structural zero is one that occurs because of a continual failure to look for the disease in question. Indeed, until healthcare practitioners become aware of a possible emerging outbreak, such zeros may be common because no one is on the lookout for that particular disease. Depending on its rarity, cases may be misdiagnosed and thus lead to falsely reported zeros. In that case, it may be advisable for health authorities to treat zero counts with caution. However they come about, the ability to account for structural zeros in addition to sampling zeros can enhance disease surveillance. In Section 2.1, we will first present the zero-inflated Poisson (ZIP) distribution, which indeed accounts for structural zeros, followed by a model for disease outbreaks based on the ZIP distribution in Section 2.2. Section 2.2.1 then presents the details for parameter inference needed for the expectation-based ZIP scan statistic presented in Section 2.3.

2.1 The zero-inflated Poisson distribution

The zero-inflated Poisson distribution is a mixture between a point mass at zero and a Poisson distribution. If the probability of drawing a zero from the point mass, i.e. a structural zero, is denoted p , and the Poisson distribution is parametrized by its expected value μ , a random variable Y following a ZIP distribution has probability mass function (pmf) (Johnson et al., 2005, p. 193)

$$\mathbb{P}(Y = y; p, \mu) = \begin{cases} p + (1 - p)e^{-\mu}, & y = 0 \\ (1 - p)\mu^y e^{-\mu}/y!, & y = 1, 2, \dots \end{cases} \quad (1)$$

The random variable $Y \sim \text{ZIP}(p, \mu)$ then has expected value $\mathbb{E}[Y] = (1 - p)\mu$ and variance $\mathbb{V}(Y) = (1 - p)\mu + p(1 - p)\mu^2$. The variance is seen to be greater than the mean, and the ZIP distribution is thus able to account for overdispersion caused by excess zeros, relative to the ordinary Poisson distribution. The next section shows how the ZIP distribution can be used to model outbreaks involving structural zeros.

2.2 A Space-Time ZIP Outbreak Model

We consider a scenario in which disease cases $Y_{it} \sim \text{ZIP}(p_{it}, \mu_{it})$ are reported at regular intervals of time $t \in \mathbb{Z}$ from locations enumerated $i = 1, \dots, n$. The intervals of time may for example be hours, days or weeks, and the locations

correspond to regions within which counts are aggregated. For example, a location may be a district in a country, and all individual disease cases that are diagnosed in that district within say a week are reported for the district as a whole. The observed data for the time period under surveillance consists of counts $\{y_{it}\}$, where $i = 1, \dots, n$ and $t = 1, \dots, T$. In our notation, time is counted backwards, so that $t = 1$ denotes the most recent time interval and T the interval at the start of the study period. Additionally, we suppose that enough data from past non-outbreak conditions exists for us to reliably estimate the parameters (p_{it}, μ_{it}) of the ZIP distribution. This is a separate task from the calculation of the scan statistic, and may involve fitting a ZIP regression model using e.g. the EM algorithm (Lambert, 1992). The global null hypothesis is that no disease outbreak is occurring in any of the locations $i = 1, 2, \dots, n$ during the study period $t = 1, 2, \dots, T$, which translates to the statement that the counts Y_{it} are independently ZIP-distributed with the parameters (p_{it}, μ_{it}) estimated from the historical data. Formally,

$$H_0 : Y_{it} \sim \text{ZIP}(p_{it}, \mu_{it}) \quad \text{for } i = 1, \dots, n \text{ and } t = 1, \dots, T.$$

If an outbreak occurs, we suppose that this happens according to a so called *hotspot* model (see e.g. Tango et al., 2011), in which the Poisson expected value parameter μ_{it} is increased by a factor $q_W > 1$ (the *relative risk*) for counts inside a given space-time window $W = (Z, D)$. Here, the *zone* Z is a collection of locations representing the spatial extent of the cluster, and D similarly designates the cluster's temporal component.

For such a window W , the alternative hypothesis may be stated

$$H_1(W) : Y_{it} \sim \begin{cases} \text{ZIP}(p_{it}, q_W \mu_{it}), & (i, t) \in W \\ \text{ZIP}(p_{it}, \mu_{it}), & (i, t) \notin W. \end{cases}$$

The problem is that the window W is unknown: we know neither the duration of the outbreak nor which locations are affected. However, because we are only interested in detecting ongoing outbreaks, we limit the investigation to windows W with temporal components $D = (1, 2, \dots, d)$ stretching from the present ($t = 1$) to $d \leq T$ units into the past, where T is the maximum outbreak duration we are willing to consider. Similarly, we are mainly interested in detecting *localized* outbreaks, for which the affected locations are close to one another spatially. This restriction can be achieved by investigating only a pre-defined set of zones \mathcal{Z} fulfilling such a condition. Given these zones, we have a collection \mathcal{W} of space-time windows W to test the above alternative hypothesis on.

One way of constructing the set of zones \mathcal{Z} is to consider each location and its k nearest neighbors (k -NN) as a zone, for $k = 0, 1, \dots, K_{\max}$. Here,

K_{\max} may be determined by not letting any zone include more than half of all locations, for example. This set can be enriched, for example by considering connected subsets of these k -NN zones (Tango and Takahashi, 2005). Other approaches are possible, both those specified independently of the response data, and those created by a more data-driven approach (as in Neill, 2012). To determine the proximity of locations, distances can be calculated between them. For example, if locations correspond to districts, then the geographical distance between the largest cities in each of two districts can serve as a distance measurement.

To see the use of a scan statistic for the above outbreak model, consider the outbreak in the set of locations corresponding to the darkly shaded regions in Figure 1. If the expanding k -nearest neighbor method described above is used to construct the set of potential outbreak zones, no zone capturing the true outbreak locations could avoid capturing the middle location with a structural zero reported for the current time period. Zones like this one would be penalized by scan statistics that do not account for structural zeros, such as those based on a simple Poisson model for counts. In contrast, a zero count will be a natural part of an outbreak cluster for a scan statistic based on the ZIP outbreak model above, and therefore not penalized. In the next section, we construct such a scan statistic based on the likelihood function implied by the model.

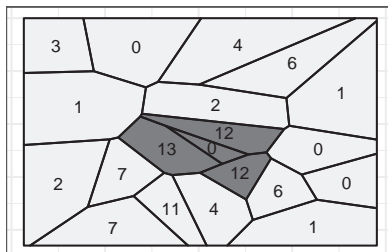


Figure 1: Example of an outbreak zone (dark shade) containing a structural zero in the center location, at a given timepoint. The numbers in the figure indicate the observed count in a given time period.

2.2.1 Likelihood Specification

The assumption that the parameters (p_{it}, μ_{it}) are known, but in practice replaced by point estimates $(\hat{p}_{it}, \hat{\mu}_{it})$ based on past data, means that the likelihood function is constant under the null hypothesis. Under the alternative hypothesis of an outbreak in a space-time window W , the likelihood $L(q_W | \{\mu_{it}\}, \{p_{it}\})$ is a function of the relative risk q_W . Unlike the case for

an ordinary Poisson distribution, such as that in Neill et al. (2005), there is no analytical solution for the likelihood-maximizing value of q_W for the zero-inflated Poisson outbreak model. A solution can instead be obtained numerically, e.g. by an expectation-maximization (EM) algorithm (Dempster et al., 1977). A similar algorithm was given for a population-based ZIP scan statistic in Cançado et al. (2014), which was formulated for a different setting and outbreak model; these differences will be clarified after the definition of the scan statistic in Section 2.3. To derive an EM algorithm for estimating q_W , we will first take a look at the complete data likelihood function, i.e. when it is known which zeros are structural zeros. To this end, let δ_{it} be an indicator variable that takes the value 1 if the count at location i and time t is a structural zero, and the value 0 if it is not. By the description of the zero-inflated Poisson distribution given previously, it follows that $\mathbb{P}(\delta_{it} = 1) = p_{it}$, and that the conditional pmf for a count at location i and time t is described by the probabilities

$$\mathbb{P}(Y_{it} = y_{it} | \delta_{it} = 0) = \exp(-q_W \mu_{it}) (q_W \mu_{it})^{y_{it}} / y_{it}!, \quad y_{it} = 0, 1, \dots,$$

and with $\mathbb{P}(Y_{it} = 0 | \delta_{it} = 1) = 1$. This holds under the alternative hypothesis $H_1(W)$ for a given space-time window W . For locations and times outside of W , or under the null hypothesis, the corresponding probabilities are obtained by setting $q_W = 1$ above. Supposing that the values of the structural zero indicators are known, we can express the complete information likelihood corresponding to the alternative hypothesis $H_1(W)$ as

$$L(q_W | \{\mu_{it}\}, \{p_{it}\}, \{\delta_{it}\}) \propto \exp \left(\sum_{(i,t) \in W} (1 - \delta_{it}) [y_{it} \log(q_W) - q_W \mu_{it}] \right). \quad (2)$$

In a practice, the structural zero indicators δ_{it} may not be known, but they can be estimated by their conditional expected values, provided the parameter q_W is known. Vice versa, the analytical maximum likelihood estimate of $q_W > 1$ can easily be calculated if the structural zero indicators are available. This suggests that an iterative solution for the maximum likelihood estimate: For each space-time window W , first initialize the relative risk q_W at its value under the null hypothesis, $q_W^{(0)} = 1$. Then for $k \geq 1$, repeat the following steps until convergence of the (incomplete information) likelihood $L(q_W | \{\mu_{it}\}, \{p_{it}\})$:

- **Expectation step:** for all pairs $(i, t) \in W$ for which $y_{it} = 0$, set

$$\hat{\delta}_{it}^{(k)} = \frac{p_{it}}{p_{it} + (1 - p_{it}) \exp(-\hat{q}_W^{(k-1)} \mu_{it})}. \quad (3)$$

For those $(i, t) \in W$ for which $y_{it} > 0$, set $\hat{\delta}_{it} = 0$ at the first iteration and leave this unchanged.

- **Maximization step:** set

$$\hat{q}_W^{(k)} = \max \left\{ 1, \frac{\sum_{(i,t) \in W} y_{it}}{\sum_{(i,t) \in W} \mu_{it} (1 - \hat{\delta}_{it}^{(k)})} \right\}, \quad (4)$$

and increase k by 1.

For a predetermined $\epsilon > 0$, the relative convergence criterion $|L(\hat{q}_W^{(k)})/L(\hat{q}_W^{(k-1)}) - 1| < \epsilon$ is used to decide when to terminate the iterations, at which point the optimal value \hat{q}_W is available. The right hand side of Equation (4) shows that observations that are likely to be structural zeros contributes positively to the relative risk estimate by reducing the influence of the corresponding Poisson mean parameter μ_{it} in the denominator; this would not be the case in the standard Poisson outbreak model.

For each space-time window W , a log-likelihood ratio statistic is then calculated as

$$\lambda_W = \log \left(\frac{L(\hat{q}_W | \{\hat{p}_{it}\}, \{\hat{\mu}_{it}\})}{L(1 | \{\hat{p}_{it}\}, \{\hat{\mu}_{it}\})} \right) = \log \left(\frac{\prod_{i,t} \mathbb{P}(Y_{it} = y_{it}; \hat{p}_{it}, \hat{q}_W \hat{\mu}_{it})}{\prod_{i,t} \mathbb{P}(Y_{it} = y_{it}; \hat{p}_{it}, \hat{\mu}_{it})} \right). \quad (5)$$

2.3 The Expectation-based ZIP Scan Statistic

Because the cardinality of \mathcal{W} can be in the range of thousands or hundreds of thousands for typical applications, a multiple testing problem would arise if each hypothesis test was conducted without adjustment for the other tests. On the other hand, a Bonferroni-type correction for the significance level would mean that only very rare events would be detected (Abdi, 2007). This may preclude small- to medium-sized outbreaks from detection. The solution suggested by Kulldorff and Nagarwalla (1995) is to focus on the cluster W which gives the largest value of the statistic λ_W . The proposed scan statistic and corresponding most likely cluster (MLC) are thus given by

$$\lambda^* = \max_{W \in \mathcal{W}} \lambda_W \quad \text{and} \quad W^* = \arg \max_{W \in \mathcal{W}} \lambda_W.$$

Because the distribution of the scan statistic is unavailable in closed form, hypothesis testing cannot be carried out using plug-in formulas. An often used alternative is to calculate a P -value by Monte Carlo simulation, as suggested by Kulldorff and Nagarwalla (1995). This procedure can be summarized as follows.

1. Determine the scan statistic λ_{obs}^* on the observed data, along with the corresponding most likely cluster W^* .
2. Use the estimated baseline parameters $(\hat{p}_{it}, \hat{\mu}_{it})$ to simulate R replicate data sets for all locations i and times t in the study period.
3. Calculate a replicate scan statistic λ_j^* on each simulated data set $j = 1, \dots, R$.
4. Reject the null hypothesis of no outbreak if the Monte Carlo P -value, given by

$$P = \left(1 + \sum_{j=1}^R \mathbf{1}\{\lambda_j^* > \lambda_{\text{obs}}^*\} \right) / (1 + R) \quad (6)$$

is smaller than the chosen significance level α . Here, $\mathbf{1}$ is the indicator function.

Secondary clusters W with potential outbreaks can be found by looking at the other top order statistics of $\{\lambda_W\}_{W \in \mathcal{W}}$ and comparing their values to the simulated scan statistics. Such tests are conservative, because, e.g., the third largest observed value will be compared to the (first) largest simulated value of λ_W (Kulldorff, 1997). Typically, $R = 999$ replications are made, which means that the computational cost is increased almost a thousandfold over calculating the statistic on just the observed data. As proposed by Abrams et al. (2006), this cost can be reduced significantly by simulating only a smaller number of scan statistics and fitting a Gumbel distribution to these replicates. A P -value can then be calculated as the tail probability of the observed scan statistic for the fitted distribution. Another possibility is to use *empirical P-values*, obtained by applying Equation 6 to previously calculated values of the scan statistic, rather than simulated values. This approach may be more reliable in practice, because hypothesis testing using Monte Carlo P -values have been shown to be miscalibrated for observational data, typically requiring a much lower significance level than the nominal α to achieve the target level of false positives (Neill, 2009a).

The scan statistic proposed above (call it EB-ZIP) differs from that given by Cançado et al. (2014) (PB-ZIP) in three major ways:

1. Analyses conducted with the PB-ZIP statistic are conditional on the total observed count: to conduct hypothesis testing by Monte Carlo replication, new counts are simulated conditional on that their total equals the total seen in the original data. As shown by Tango et al. (2011), this conditioning can in a worst-case scenario ensure that no outbreak is detected, and may in general have low power to detect outbreaks that affect a large proportion of the area under surveillance

(Neill, 2009a) . On the other hand, the proposed EB-ZIP statistic does not condition on the observed total count when conducting hypothesis testing.

2. The PB-ZIP statistic uses the populations at risk for each area directly in the calculation of the scan statistic, while the relative risk and zero probability parameters are equal for all locations inside or outside a given cluster in the alternative hypothesis (and the same for all locations under the null hypothesis). The populations at risk may not always be available or even applicable, and can be harder to adjust for e.g. seasonal or day-of-week effects compared to the expected values μ_{it} (Neill, 2006). Indeed, with a sufficient amount of historical data, the parameters (p_{it}, μ_{it}) can easily be estimated in a regression-type framework.
3. The PB-ZIP statistic was introduced for a purely spatial outbreak detection scenario, which may be adequate for retrospective analyses. The method presented in this paper is designed for space-time data, suitable for prospective surveillance situations in which an outbreak may have started to emerge only during the few most recent time periods.

In brief, using the nomenclature introduced by Neill (2006), the scan statistic presented in this paper is *expectation-based*, rather than *population-based*. In the next section, we conduct a simulation study to investigate the detection abilities of the proposed scan statistic in a prospective space-time setting.

3 Simulation Study

A comprehensive simulation study was performed to test the detection timeliness and spatial accuracy of the proposed scan statistic (called EB-ZIP below). A smaller subset is illustrated below, but the conclusions put forth are drawn from the full set of simulations. For comparison, the expectation-based Poisson (EB-POI; Neill et al., 2005) and the population-based Poisson (PB-POI; Kulldorff, 2001) were also calculated. Following an initial period of 9 weeks with ZIP-distributed data simulated from non-outbreak conditions at $n = 100$ randomly placed locations, outbreaks with different relative risks were simulated for 11 consecutive weeks at specified subsets of the locations. Thus the temporal window of each scan statistic covered an increasing amount of outbreak data for each new week scanned. The maximum outbreak duration considered was $T = 10$ weeks, which is the same maximum duration used in Section 4. An outbreak was defined as detected in the first week for which the calculated P -value fell below a given significance level α . A range of different values of α were tried, in order to evaluate the sensitivity of the

detection timeliness, spatial accuracy and false positive rate with respect to the significance level. The zones used in the analysis were constructed by the nearest-neighbor method described in Section 2.2, and contained at most 25 locations each. Multiple outbreak *scenarios* were considered, defined by all possible combinations of the following parameters:

- The baseline ZIP count parameter: $\mu_{it} = \mu \in \{1, 5, 10\}$.
- The baseline structural zero probability: $p_{it} = p \in \{0.01, 0.05, 0.15, 0.25, 0.5\}$.
- The outbreak relative risk: $q_W \in \{1, 1.1, 1.25, 1.5, 2\}$.
- The spatial extent of the outbreak: either 5 or 20 locations.

The value $q = 1$ corresponds to a non-outbreak and serves as a check of the false positive rate of each method. For each outbreak scenario, 1000 outbreaks were simulated and scan statistics calculated on each. Additionally, 999 non-outbreaks were simulated for each set of baseline parameters (p, μ) , to allow for P -value calculations and hypothesis testing. Because the difference between Monte Carlo and Monte Carlo + Gumbel P -values was deemed to be sufficiently small, only the latter type of P -value was used in the analysis.

To evaluate the spatial accuracy of the ZIP scan statistic, we measured the spatial precision S_P and the spatial recall S_R as defined by Neill (2012, p. 356). Denoting by Z^* the spatial component (*zone*) of the detected space-time cluster, and Z^{true} the true outbreak zone, these measures are given by:

$$S_P = \frac{|Z^* \cap Z^{\text{true}}|}{|Z^*|}, \quad S_R = \frac{|Z^* \cap Z^{\text{true}}|}{|Z^{\text{true}}|},$$

where, for example, $|Z^*|$ denotes the number of locations contained in the zone Z^* . The spatial precision informs us about the relevance of the detected cluster, in terms of what fraction of the detected locations truly are affected by an outbreak. The recall, on the other hand, tells us what fraction of the locations truly affected by an outbreak that we captured—how well does the method avoid false negatives? There is a trade-off between precision and recall, because adding more locations to the reported cluster will eventually improve the recall, but penalize the precision. Conversely, removing locations from the reported cluster will eventually improve precision at the expense of recall, given that at least one true outbreak location is captured. As a summary of both precision and recall, the harmonic mean $F = (S_P^{-1} + S_R^{-1})^{-1}$ of the two measures can be used (Neill, 2009b). We computed these measures for each simulated outbreak, noting in particular their values at the first day for which the P -value fell below the significance level α .

3.1 Simulation Results

Before measuring the timeliness of a detection method, it is informative to first investigate its false positive rate. A method that signals a detection regardless of whether an outbreak is actually occurring will have great timeliness but is utterly useless in practice. We simulate 1000 non-outbreaks ($q_W = 1$) for each combination of baseline parameters (p, μ) , and compute the proportion of false positives ($P < \alpha$) for a range of α values. In Figure 2 we show the proportion of outbreaks detected by each scan statistic, with the significance level α ranging between 0.0001 and 0.1. The plot corresponds to the scenario with parameters $\mu = 5$ and $p = 0.15$.

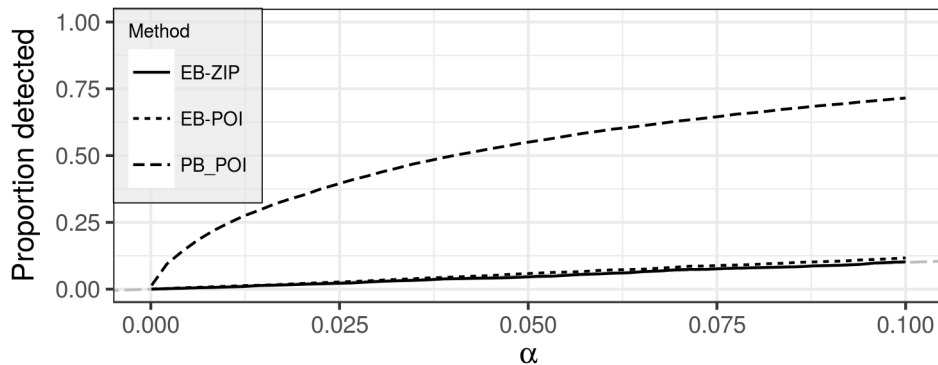


Figure 2: Proportion of outbreaks detected versus significance level for non-outbreak data. The grey dot-dashed line marks the relationship $y = x$. The figure corresponds to the scenario with parameters $p = 0.15$ and $\mu = 5$.

At a given significance level α , a detection method should on expectation preferably not give a higher proportion of false alarms than α , which is the proportion expected if the assumptions on which the method is based are true. Indeed, this is the case for the proposed EB-ZIP method, and Figure 2 shows that the line for EB-ZIP (solid black) follows the line $y = x$ (dot-dashed grey) very well. Also clear from Figure 2 is that the PB-POI method signals far more outbreaks than is expected, while the EB-POI method only signals slightly more outbreaks than EB-ZIP. For other parameter settings, not shown, it can be concluded that the proportion of false alarms of PB-POI increases rapidly with the structural zero probability p and decreases moderately with μ , although it is seemingly always higher than the nominal α . For the EB-POI method, the false alarm ratio is mostly lower than α , but the opposite is true for high values of p .

The detection timeliness of a method that does not give too many false alarms may still be irrelevant if the clusters detected do not overlap with the

actual locations affected by a disease outbreak. We therefore investigate the spatial accuracy of detected outbreaks at different significance levels α . In Figure 3(a), we show the proportion of outbreaks detected per week of the outbreak for each of the three scan statistics, for a fixed significance level $\alpha = 0.05$.

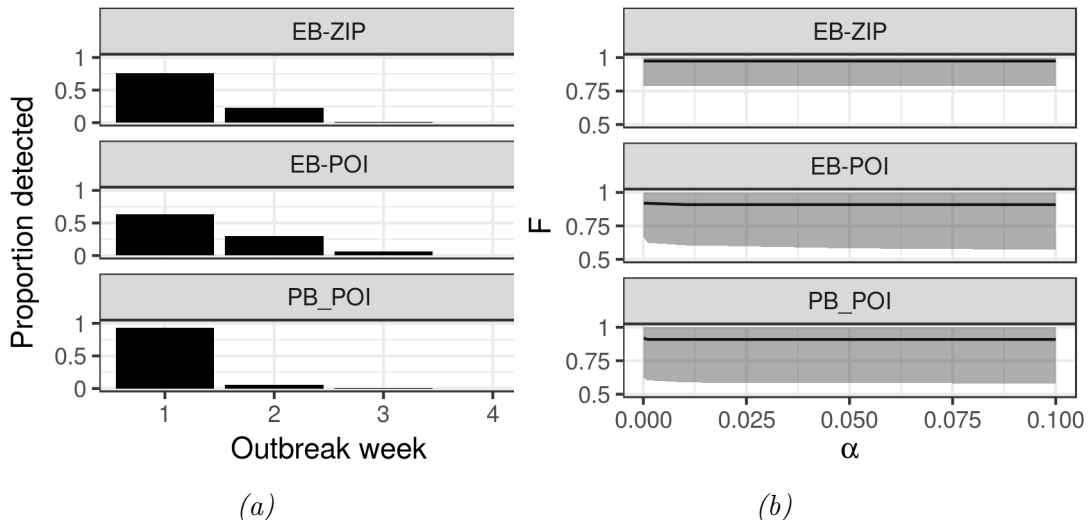


Figure 3: In (a), the proportion of outbreaks detected per week, for a fixed significance level $\alpha = 1/50$. In (b), the solid line marks the median harmonic mean F in outbreak week 3 for detected outbreaks ($P < \alpha$) for different significance levels α . The shaded regions are 90% pointwise confidence intervals for F . Parameter settings were $p = 0.15$, $\mu = 5$, $q_W = 1.5$, and the outbreak affected 20 out of 100 locations.

In this instance, most outbreaks have been detected by week 3 for each scan statistic. In Figure 3(b) the harmonic mean F defined previously is shown for varying levels of α for outbreaks detected in week 3. Clearly, the PB-POI scan statistic detects outbreaks early—even when there is not outbreak, as in Figure 2—but the 90% confidence interval for F stretches just below 0.6 to 1 for most significance levels, meaning that its spatial accuracy is somewhat erratic. The EB-ZIP scan statistic also detects outbreaks early—most of them in week 1 for these parameter settings—but matches this timeliness with a high and steady spatial accuracy.

Lastly, we examine the performance of the ZIP scan statistic as the structural zero probability approaches zero. At this limit, the ZIP distribution becomes the Poisson distribution and the performance of the EB-ZIP and PB-ZIP methods should converge. Figure 4 shows that the harmonic mean

F of all three scan statistics converge to nearly 1 when $p \rightarrow 0$; the solid line indicates the median of F over simulations, and the shaded region stretches from the 5th to the 95th percentile of F . Looking at this from the other direction, it is clear that the relative performance of the ZIP scan statistic, in terms of spatial accuracy, becomes better the larger the structural zero probability p is. The EB-POI and PB-POI methods also show more variation in F as p increases, relative to EB-ZIP.

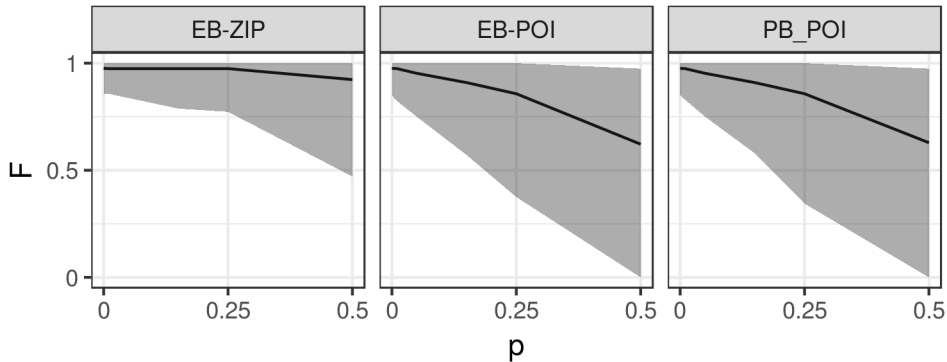


Figure 4: Median (solid line) and 90% pointwise confidence interval (shaded region) of the harmonic mean F in week 3 of the outbreak, for different values of the structural zero probability p . Parameter settings were $\mu = 5$, $q_W = 1.5$, and the outbreak affected 20 out of 100 locations.

The overall results of the simulation study indicate that the expectation-based ZIP scan statistic is able to accurately detect outbreaks in a timely manner, particularly when non-zero counts are large on average, or when structural zeros are abundant. These qualities are improved when the spatial size of the outbreak is large or when the magnitude of the outbreak, in terms of the relative risk q_W , is significant. To demonstrate what is required to apply the proposed scan statistic on real disease data, and how it may differ in the clusters reported compared to the two other scan statistics considered in this section, we next apply the ZIP scan statistic to the weekly cases of *Campylobacteriosis* in the districts of Germany.

4 Application: *Campylobacteriosis* in Germany

Campylobacteriosis is a diarrhoeal disease caused by the bacteria *Campylobacter*, with approximately 80–90% of human cases in industrialized countries attributed to the species *Campylobacter jejuni* and 5–10% attributed to

Campylobacter coli (Blaser and Engberg, 2008; Fitzgerald et al., 2008). The main route of transmission to humans is via poorly cooked meat and other meat products—particularly poultry—but also via raw or contaminated milk, and water or ice. Campylobacteriosis has one of the highest incidences among the notifiable diseases monitored by the Robert Koch Institute (RKI) in Germany. From the public database *SurvStat@RKI 2.0* (RKI, 2017), we collected the weekly number of cases of Campylobacteriosis due to *Campylobacter coli* in the years 2011–2016, for each of the 402 districts (*kreise*) of Germany, subdividing the counts for Berlin by the city’s 12 boroughs. A map of the 402 with districts shaded by incidence of Campylobacteriosis in 2016 is shown in Figure 5a. In Figure 5b, the weekly counts of Campylobacteriosis aggregated to the whole of Germany are shown for the period 2009–2016. A clear seasonal pattern with peaks in the summer months is visible here, which is not the case for the corresponding district-level plot (not shown).

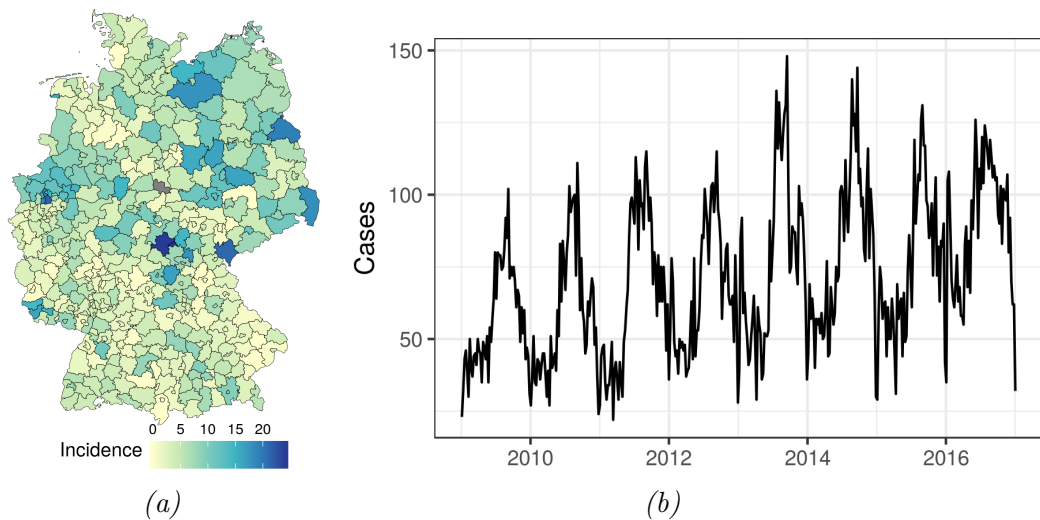


Figure 5: In (a), the incidence (new cases per 100,000 people) of Campylobacteriosis (*Campylobacter coli*) in the districts of Germany in 2016. In (b), the total number of cases per week in Germany is shown for the period 2009–2016.

Noticeable outliers in the years 2011–2015 were matched against news articles and epidemiological records from approximately the same times and places. One such outlier was found to correspond to an outbreak in the district Märkischer Kreis in January of 2013 (Südwestfalen-Nachrichten, 2013); it was replaced by the median of counts in the surrounding weeks from all the baseline years. Data from the period 2011–2015 were then used as a baseline on which a zero-inflated regression model with was fitted by maximum

likelihood. The parameters of the model were specified as

$$\begin{aligned}\log(\mu_{it}) &= \log(\text{pop}_{it}) + \alpha_\mu + \gamma_\mu \delta_i^{\text{urban}} + \theta_\mu^{\text{state}(i)} + \beta_0 \tilde{t} + f_\mu(\text{east}_i, \text{north}_i) \\ &\quad + \beta_1 \sin\left(\frac{2\pi \text{ISOweek}_t}{52.18} + \phi_1\right) + \beta_2 \sin\left(\frac{4\pi \text{ISOweek}_t}{52.18} + \phi_2\right) \\ \text{logit}(p_{it}) &= \log(\text{pop}_{it}) + \alpha_p + \gamma_p \delta_i^{\text{urban}} + \theta_p^{\text{state}(i)} + f_p(\text{east}_i, \text{north}_i),\end{aligned}$$

where \tilde{t} is a standardized measure of time; δ_i^{urban} is an indicator variable taking the value 1 if district i is classified as an urban district (*stadtkreis*) as opposed to a rural district; $\theta_\cdot^{\text{state}(i)}$ is a coefficient shared by all districts in the same federal state as district i ; pop_{it} is the estimated population of district i at time t (used as an offset); the two sine terms representing seasonal fluctuations over the course of a year, using a period of 52.18 weeks instead of 52 to account for leap weeks; and f_μ and f_p are smooth functions of the coordinates of each location, represented by thin plate regression spline bases (Wood, 2003) with a basis dimension of 150 in each case. The form of the model and the basis dimensions were arrived at by minimization of AIC over a finite set of models using functions from the R packages `pscl` (Zeileis et al., 2008) and `mgcv` (Wood, 2003). A Poisson GLM was also fit with the same form of μ_{it} as above, to use for the expectation-based Poisson scan statistic. For our analysis, we considered outbreaks with a maximum duration of 10 weeks, which was the maximum reporting delay found to be relevant by Salmon et al. (2015), and the investigated spatial zones had the flexible shape proposed by Tango and Takahashi (2005) with at most 10 districts in each zone. This yielded a total of 53,830 spatial zones and thus ten times as many potential space-time clusters. For hypothesis testing, we calculated scan statistics for each week of the baseline data and used these values in Equation (6) to obtain empirical P -values, for reasons discussed in Section 2.3. These were calculated using a 10 week rolling window and the same spatial zones used for the test period. Unfortunately, because the population-based Poisson scan statistic conducts its analysis based on the value of the total observed count, there are too few values of the statistic in the baseline period to match those in the study period. Therefore, Monte Carlo P -values had to be used for this method.

Data from 2016 were analyzed using the proposed expectation-based ZIP statistic (EB-ZIP), the expectation-based Poisson statistic (EB-POI) and the population-based Poisson statistic (PB-POI). This yielded scan statistics calculated in weeks 9–51 of that year. The PB-POI scan statistic consistently reported very low P -values ($< 10^{-4}$) throughout the period; this tendency to signal a detection (for common nominal significance levels) was also seen in the simulation study. The two expectation-based scan statistics, on the

other hand, generally report low P -values (< 0.05) in weeks 9–31, and mostly higher values in the following period. These scan statistics also tend to find clusters that are smaller in the spatial dimension (median of 5 locations for EB-ZIP; 6 for EB-POI) than PB-POI (median 10 locations, which is the maximum). In Figure 6, we show the spatial component (zones) of the most likely cluster reported by each scan statistic in week 12 of 2016. All these zones lie in the state of North Rhine-Westphalia, although only one district, Unna, is reported by all three methods. The remainder of the 10 districts reported by the PB-ZIP method lie to the west of Unna, while those of the EB-ZIP method lie more to the north-east and are fully engulfed by the 8 districts reported by the EB-POI method. The P -values reported by the EB-ZIP, EB-POI and PB-POI methods are approximately 0.07, 0.1 and $2 \cdot 10^{-5}$, respectively. Although the number of cases in week 12 were fairly low overall, multiple districts captured in the cluster of each statistic had shown counts of 3 and above in the previous few weeks, something not seen to the same extent in the same period in earlier years.

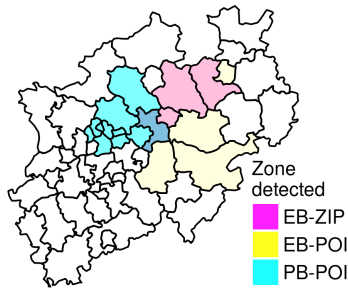


Figure 6: Map of the districts of North Rhine-Westphalia, in which the zones reported by each scan statistic in week 12 of 2016 are colored.

Reported outbreak durations are more similar however, with a median reported duration of 10 weeks for EB-POI and PB-POI, and 9 weeks for EB-ZIP. Perhaps of more interest is the degree of overlap between the spatial components of the reported most likely clusters of each method. Defining the spatial overlap as the fraction of locations in common out of the total reported for a pair of the methods, the average overlap between the EB-ZIP and EB-POI methods was 61%, while only 26% between EB-ZIP and PB-POI. Between EB-POI and PB-POI, it was 34%. Upon closer inspection, it seems that all clusters reported by the PB-POI method lies in the state of North Rhine-Westphalia, which is the most populous state of Germany. The EB-ZIP method, on the other hand, reports clusters across 7 states, many in the west, south-west and south of Germany, and the EB-POI method reports

clusters across 5 states with similar geographical characteristics. In terms of outbreaks, this paints a different picture than the incidence rates shown in Figure 5a, which are generally high in the north-east and low in the south and south-west. Despite the low P -values reported by the three scan statistics in many of the weeks of the study period, no ‘significant’ result could be matched to events described in news articles and epidemiological records for the same time period. As a check, we also ran the three scan statistics on the single-district outbreak in January of 2013 mentioned earlier. This outbreak was found in the MLCs reported by the EB-ZIP and EB-POI methods, but not that of the PB-POI method. The lack of data on confirmed clusters is a situation frequently met in evaluating new detection methods. For example, in disease surveillance a more systematic investigation of cases using decision support methods is often needed, but this does not always result in data directly amenable for cluster analysis. Nevertheless, the proposed method and accompanying R package could be integrated into such a decision support system to help guide the search efforts and ensure that no important outbreaks are missed.

5 Conclusions

An excess of zero counts in public health data may cause scan statistics based on the Poisson distribution to perform suboptimally. In addition, many traditional scan statistics estimate baseline parameters from the very data that they attempt to detect outbreaks in. Critics argue that these parameters ought instead to be estimated on historical data that does not overlap with the data under investigation, and that analyses made should not be conditional on the observed total count (Tango et al., 2011; Tango, 2016). In this paper, we have proposed an expectation-based scan statistic for zero-inflated Poisson data that addresses these issues. By way of simulation, we have shown that the method performs well under a range of conditions. In particular, the proposed ZIP scan statistic performs well relative to two scan statistics based on a simple Poisson model, under conditions in which non-zero counts are distant from zero, or in which structural zeros are abundant. The detection power, both in terms of spatial accuracy and timeliness of detection, improves with the size and length of the outbreak, as well as its effect on raising counts above their baseline. To demonstrate the scan statistic, we applied it to weekly cases of Campylobacteriosis in the districts of Germany. This analysis served to illustrate some of the qualitative differences of the results reported by the proposed method and two alternative scan statistics.

Apart from an excess of zeros, real-world data is often characterized by a greater variation in the non-zero counts than would be expected under the assumption of Poisson- or ZIP-distributed counts. Recent work by de Lima et al. (2015) considers population-based scan statistics for the overdispersed Poisson and double Poisson distributions. A possible extension of the work in this paper may thus be to derive the corresponding expectation-based scan statistics for these two distributions. The methods used in this paper are provided in the free and open-source R package `scanstatistics`, available from CRAN (Allévius, 2017).

Acknowledgements

The authors thank Martin Sköld for constructive feedback during the writing of this article. The authors also acknowledge financial support from the Swedish Research Council (Grant 2013:05204, Grant 2015-05182_VR).

References

- Abdi, H. (2007). The Bonferroni and Šidák corrections for multiple comparisons. In Salkind, N. J., editor, *Encyclopedia of Measurement and Statistics*. SAGE Publications, Inc., Thousand Oaks, CA.
- Abrams, A. M., Kulldorff, M., and Kleinman, K. (2006). Empirical/asymptotic P -values for Monte Carlo-based hypothesis testing: An application to cluster detection using the scan statistic. *Advances in Disease Surveillance*, 1(1).
- Allévius, B. (2017). *scanstatistics: Space-time anomaly detection using scan statistics*. R package version 1.0.
- Blaser, M. J. and Engberg, J. (2008). Clinical aspects of campylobacter jejuni and campylobacter coli infections. In Nachamkin, I., Szymanski, C. M., and Blaser, M. J., editors, *Campylobacter*, chapter 6, pages 99–121. ASM Press, Washington D.C., 3 edition.
- Cakici, B., Hebing, K., Grünewald, M., Saretok, P., and Hulth, A. (2010). CASE: a framework for computer supported outbreak detection. *BMC Medical Informatics and Decision Making*, 10(14).
- Cançado, A. L. F., da Silva, C. Q., and da Silva, M. F. (2014). A spatial scan statistic for zero-inflated Poisson process. *Environmental and Ecological Statistics*, 21(4):627–650.

- Correa, T. R., Assunção, R. M., and Costa, M. A. (2015a). A critical look at prospective surveillance using a scan statistic. *Statistics in Medicine*, 34(7):1081–1093.
- Correa, T. R., Assunção, R. M., and Costa, M. A. (2015b). Response to commentary on 'A critical look at prospective surveillance using a scan statistic'. *Statistics in Medicine*, 34(7):1096.
- de Lima, M. S., Duczmal, L. H., Neto, J. C., and Pinto, L. P. (2015). Spatial scan statistics for models with overdispersion and inflated zeros. *Statistica Sinica*, 25(1):225–241.
- Dempster, A. P., Laird, N. M., and Rubin, D. B. (1977). Maximum likelihood from incomplete data via the EM algorithm. *Journal of the Royal Statistical Society, Series B (Statistical Methodology)*, 39(1):1–38.
- Fitzgerald, C., Whichard, J., and Nachamkin, I. (2008). Diagnosis and antimicrobial susceptibility of campylobacter species. In Nachamkin, I., Szymanski, C. M., and Blaser, M. J., editors, *Campylobacter*, chapter 12, pages 227–243. ASM Press, Washington D.C., 3 edition.
- Gangnon, R. E. and Clayton, M. K. (2001). A weighted average likelihood ratio test for spatial clustering of disease. *Statistics in Medicine*, 20(19):2977–2987.
- Haselbach, A.-C. (2013–01–15). Keimbelastung im Trinkwasser von Landhausen und Stübecken in Hemer geht zurück. *Südwestfalen-Nachrichten*.
- Johnson, N. L., Kemp, A. W., and Kotz, S. (2005). *Univariate discrete distributions*. Wiley, 3 edition.
- Kleinman, K. (2015). *rsatscan: Tools, Classes, and Methods for Interfacing with SaTScan Stand-Alone Software*. R package version 0.3.9200.
- Kulldorff, M. (1997). A spatial scan statistic. *Communications in Statistics - Theory and Methods*, 26(6):1481–1496.
- Kulldorff, M. (2001). Prospective time periodic geographical disease surveillance using a scan statistic. *Journal of the Royal Statistical Society, Series A (Statistics in Society)*, 164:61–72.
- Kulldorff, M. (2016). Satscan™.

- Kulldorff, M. and Kleinman, K. (2015). Comments on 'A critical look at prospective surveillance using a scan statistic' by T. Correa, M. Costa, and R. Assunção. *Statistics in Medicine*, 34(7):1094–1095.
- Kulldorff, M. and Nagarwalla, N. (1995). Spatial disease clusters: Detection and inference. *Statistics in Medicine*, 14(8):799–810.
- Lambert, D. (1992). Zero-inflated Poisson regression, with an application to defects in manufacturing. *Technometrics*, 34(1):1–14.
- Li, X. Z., Wang, J. F., Yang, W. Z., Li, Z. J., and Lai, S. J. (2011). A spatial scan statistic for multiple clusters. *Mathematical Biosciences*, 233(2):135–142.
- Minamisava, R., Nouer, S. S., de Moraes Neto, O. L., Melo, L. K., and Andrade, A. L. S. (2009). Spatial clusters of violent deaths in a newly urbanized region of Brazil: Highlighting the social disparities. *International Journal of Health Geographics*, 8(66).
- Moni Bidin, C., de la Fuente Marcos, R., de la Fuente Marcos, C., and Carraro, G. (2009). Not an open cluster after all: the NGC 6863 asterism in Aquila. *Astronomy & Astrophysics*, 510.
- Neill, D. B. (2006). *Detection of spatial and spatio-temporal clusters*. Phd thesis, Carnegie Mellon University.
- Neill, D. B. (2009a). An empirical comparison of spatial scan statistics for outbreak detection. *International Journal of Health Geographics*, 8(20).
- Neill, D. B. (2009b). Expectation-based scan statistics for monitoring spatial time series data. *International Journal of Forecasting*, 25(3):498–517.
- Neill, D. B. (2012). Fast subset scan for spatial pattern detection. *Journal of the Royal Statistical Society, Series B (Statistical Methodology)*, 74(2):337–360.
- Neill, D. B., Moore, A. W., Sabhnani, M., and Daniel, K. (2005). Detection of emerging space-time clusters. *Proceeding of the eleventh ACM SIGKDD international conference on Knowledge discovery in data mining - KDD '05*, page 218.
- Robert Koch Institute (2017). SurvStat@RKI 2.0. data retrieved 2017-02-10.

- Salmon, M., Schumacher, D., Burmann, H., Frank, C., Claus, H., and Höhle, M. (2016a). A system for automated outbreak detection of communicable diseases in Germany. *Eurosurveillance*, 21(13):30180.
- Salmon, M., Schumacher, D., and Höhle, M. (2016b). Monitoring count time series in R: Aberration detection in public health surveillance. *Journal of Statistical Software*, 70(1):1–35.
- Salmon, M., Schumacher, D., Stark, K., and Höhle, M. (2015). Bayesian outbreak detection in the presence of reporting delays. *Biometrical Journal*, 57(6):1051–1067.
- Tango, T. (2016). On the recent debate on the space-time scan statistic for prospective surveillance. *Statistics in Medicine*, 35(11):1927–1928.
- Tango, T. and Takahashi, K. (2005). A flexibly shaped spatial scan statistic for detecting clusters. *International Journal of Health Geographics*, 4(11):15.
- Tango, T., Takahashi, K., and Kohriyama, K. (2011). A space-time scan statistic for detecting emerging outbreaks. *Biometrics*, 67(1):106–115.
- Tuia, D., Ratle, F., Lasaponara, R., Telesca, L., and Kanevski, M. (2008). Scan statistics analysis of forest fire clusters. *Communications in Nonlinear Science and Numerical Simulation*, 13(8):1689–1694.
- Wood, S. (2003). Thin plate regression splines. *Journal of the Royal Statistical Society, Series B (Statistical Methodology)*, 65(1):95–114.
- Zeileis, A., Kleiber, C., and Jackman, S. (2008). Regression models for count data in R. *Journal of Statistical Software*, 27(8).